

Journal of Materials Chemistry B

Accepted Manuscript



This is an *Accepted Manuscript*, which has been through the Royal Society of Chemistry peer review process and has been accepted for publication.

Accepted Manuscripts are published online shortly after acceptance, before technical editing, formatting and proof reading. Using this free service, authors can make their results available to the community, in citable form, before we publish the edited article. We will replace this *Accepted Manuscript* with the edited and formatted *Advance Article* as soon as it is available.

You can find more information about *Accepted Manuscripts* in the [Information for Authors](#).

Please note that technical editing may introduce minor changes to the text and/or graphics, which may alter content. The journal's standard [Terms & Conditions](#) and the [Ethical guidelines](#) still apply. In no event shall the Royal Society of Chemistry be held responsible for any errors or omissions in this *Accepted Manuscript* or any consequences arising from the use of any information it contains.

Cite this: DOI: 10.1039/c0xx00000x

www.rsc.org/xxxxxx

ARTICLE TYPE

Enhanced chemotherapy efficacy by co-delivery of shABCG2 and doxorubicin with a pH-responsive charge-reversible layered graphene oxide nanocomplex

Yuling He¹, Lifen Zhang^{1*}, Zhenzhen Chen¹, Yong Liang², Yushun Zhang¹, Yanli Bai³, Jing Zhang³, Yanfeng Li¹

Abstract: In this study, we constructed layered graphene oxide (GO) nanocomplex with pH-responsive charge-reversible chitosan-aconitic anhydride (CS-Aco), biocompatible polyethylene glycol (PEG) and low molecular weight polyethylenimine (PEI), and employed them as a novel delivery system for intracellular pH-triggered DOX and short hairpin RNA (shRNA) controlled release and synergistic therapy. The nanocomplex GO-PEI-PEG/DOX/CS-Aco/PEI/shRNA exhibited high drug and shRNA loading, and good stability at physiological pH. In an acid pH environment, the negatively charged layer CS-Aco hydrolyzed into positively charged chitosan, causing the shielding layers of the nanocomposite to loosen. The disassembled GO-PEI-PEG/DOX and chitosan efficiently ruptured the endosome, significantly facilitating the release of DOX and PEI/shRNA into the cytoplasm, and then shRNA disassembled rapidly because of their weak electrostatic interactions with the short PEI chains. Consequently, GO-PEI-PEG/DOX/CS-Aco/PEI/shRNA exhibited excellent shABCG2 and DOX co-delivery efficiency of the HepG2 cells, better than GO/DOX and non-charge-reversible GO-PEI-PEG/DOX/CS-Car/PEI/shRNA nanocomplex. Furthermore, these novel nanocomplexes have high efficiency in silencing ABCG2 expression, and exhibited a significant synergistic efficacy of chemotherapy.

Keywords: GO nanoparticle; pH-responsive; charge-reversible; co-delivery; polyethylenimine

Introduction

The RNA interference (RNAi) technique is a promising therapeutic approach for cancer gene therapies in which protein expression is suppressed by targeted cleavage of messenger RNA (mRNA), and the technique has been intensively investigated since gene knockdown was first demonstrated in mammalian cells.¹ Compared with widely used short interfering RNA (siRNA), plasmid-expressed short hairpin RNA (shRNA) constructs are a more important gene silencing tool for long-term, stable knockdown of gene expression, offering significant potential in overcoming multiple drug resistance (MDR) in the cancer cells. Target gene ABCG2 has been cloned into the shRNA vector because it is highly expressed in various cancer cells, especially drug-resistant cancer cells.² The retroviral vectors have been used for the delivery of shABCG2 into many cancer cell types to knock down specific genes and improve the sensitivity of cancer cells to anticancer drugs.³ Although these the retroviral systems have been found to be efficient, their safety and synergistic therapy efficacy with anticancer drugs remains one of barriers for in vivo application.

Synergistic gene and drug therapy is a promising strategy for treating cancer. However, there are still several problems to overcome in delivering drugs and shRNA to an appropriate site.

For example, low drug loading capacity of carriers, difficulty with the passive entry of carriers into cells, inefficient endosomal escape and subsequent release of shRNA from nanocarriers, which necessitates delivery via a suitable and safer carrier. Smart nanocarriers that are responsive to external stimuli such as heat, glutathione, light, pH or magnetic fields are necessary for controlled release of genes or drugs at suitable sites.⁴⁻⁸ Although the endocytic pathway begins near a physiological pH of 7.4, it drops to pH 5.5–6.0 in endosomes, and approaches pH 5.0 in lysosomes.⁹⁻¹¹ Thus, pH-sensitive delivery systems are important for avoiding undesired release of the anticancer drug or gene in the blood stream and to improve effective release of the therapeutic agents in the tumor tissue or tumor cells.

Herein, we use the layer-by-layer method to fabricate a co-delivery system for shABCG2 and the anticancer drug doxorubicin (DOX) from graphene oxide (GO) functionalized with polyethylene glycol (PEG), polyethylenimine (PEI), and chitosan aconitic anhydride (CS-Aco), which is pH-responsive and charge-reversible, to obtain GO-PEI-PEG/DOX/CS-Aco/PEI/shABCG2. GO was chosen because of its good biocompatibility, high drug loading capacity, and adsorption of aromatic drug molecules through π - π stacking and hydrophobic interactions.¹²⁻¹⁵ Cationic polymers, such as PEI, are particularly effective for gene and shRNA delivery because they can

condense the gene and facilitate the endosomal escape of the cargo molecules, enabling effective cellular internalization. Negatively charged CS-Aco is a pH-responsive charge-reversible polymer that binds tightly to positively charged GO-PEI-PEG/DOX and PEI/shABCG2 at a pH of 7.4, and is hydrolyzed to positively charged CS at acidic pH. The combination of GO-PEI-PEG, PEI, and CS-Aco is expected to allow DOX and shABCG2 to be loaded at physiological pH, efficiently released at acid pH through electrostatic repulsion, and then improve the sensitivity of cancer cells to anticancer drugs by efficiently silencing the specific genes ABCG2. The schematic illustration of GO-PEI-PEG/DOX/CS-Aco/PEI/shABCG2 nanocarrier for intercellular co-delivery of shABCG2 and DOX into cancer cells is shown in Scheme 1.

We demonstrate that the pH-triggered charge-reversible nanocomplex GO-PEI-PEG/DOX/CS-Aco/PEI/shABCG2 is an excellent nanocarrier for effective delivery of shRNA and DOX, and that the co-delivery of shABCG2 and DOX by the nanocarrier into cancer HepG2 cells exhibits a synergistic effect, which significantly enhances chemotherapy efficacy. To the best of our knowledge, this is the first report of a pH responsive charge-reversible GO-based nanocarrier for co-delivering shABCG2 and DOX into cancer cells.

Materials and methods

Materials

Graphite powder with an average particle size of 30 μm was purchased from Sinopharm Chemical Reagent Co., Ltd (Shanghai, China). 3-(4,5-dimethylthiazol-2-yl)-5-(3-carboxymethoxyphenyl)-2-(4-sulfophenyl)-2H-tetrazolium, inner salt (MTS), cis-aconitic anhydride, tricarballic acid, polyethyleneimine (PEI, M_w 25 kDa, 1.2 kDa), Doxorubicin hydrochloride (DOX), N-(3-dimethylaminopropyl)-N'-ethylcarbodiimide hydrochloride (EDC) and N,N'-dicyclohexylcarbodiimide (DCC) were obtained from Sigma-Aldrich Co. N-hydroxysuccinimide (NHS) was purchased from Kefeng Chemical Reagent Co., Ltd (Shanghai, China). 4, 6-Diamidino-2-phenylindole dihydrochloride (DAPI) was from Bioworld Technology Co., Ltd. Water-solution chitosan was obtained from Jinan Haidebei Marine Bioengineering Co., Ltd. Monomethylether polyethylene glycol (mPEG, M_w 1.9 kDa) was purchased from Alfa Aesar. Dulbecco's Modified Eagle's Medium (DMEM), fetal bovine serum (FBS) and YOYO-1 iodide (1 mM solution in DMSO) were obtained from Invitrogen. HepG2 cells were kindly provided by Dr. Li (University of Lanzhou). Mouse monoclonal ABCG2 antibody and Alexa-Fluor-488-conjugated donkey anti-mouse IgG antibody were from Molecular Probes (Eugene, OR). ABCG2 shRNA (shABCG2) and control scrambled shRNA were designed and purchased from Sangon Company (Shanghai, China) and each was cloned into the pSicoR shRNA vector. All other chemicals reagents were analytical grade and obtained from commercial sources.

Preparation of GO

GO was prepared from natural graphite powder through the modified Hummers method.¹⁶ In a typical synthesis, a mixture of 3.75 g of graphite and 3.75 g of NaNO_3 were added to 180 mL of

98% H_2SO_4 by stirring at the ice-bath over a period of 0.5 h. Subsequently, 22.5 g of KMnO_4 was introduced into the mixture and stirred while keeping the temperature below 20 $^\circ\text{C}$. The mixture was then heated to 35 $^\circ\text{C}$ and continuously stirred for 3 h. After that, 750 mL of 3% H_2O_2 was slowly dropped to the solution, giving rise to a pronounced exothermal effect up to 98 $^\circ\text{C}$ by stirred for 1 h. The solution was washed three times with 10% of HCl by centrifugation and repeatedly with deionized water until pH of 6-7. Next, the result of graphite oxide powder was dispersed in the deionized water and ultra-sonicated for 8 h to exfoliate into graphene oxide (GO) sheets. Then the suspension was centrifuged at 3700 rpm for 30 min and the solid was discarded. Finally, the sample was freeze-dried to obtain the GO solid.

Preparation of GO-PEI-PEG

The monomethylether PEG was modified to a carboxyl-terminated intermediate by esterification with cyclic aliphatic anhydride according to the literature report.¹⁷ In brief, 2.5 g of pre-dried mPEG was dissolved in 20 mL of water-free toluene, 0.64 g of maleic anhydride was added under the protection of argon. The solution was continuously stirred at 70 $^\circ\text{C}$ for 48 h under an argon atmosphere. Toluene and the excess maleic anhydride were then eliminated by distillation and sublimation at 40 $^\circ\text{C}$ under vacuum. Next, 1.07 g of the intermediate mentioned above together with 0.31 g of NHS was dissolved in 20 mL water free dichloromethane. Then the reaction mixture was cooled in an ice-water bath and 0.54 mmol of DCC was added under argon. The reaction system was stirred for 1 h at 0 $^\circ\text{C}$ under argon, and further 24 h at room temperature. The precipitated 1, 3-dicyclohexylurea (DCU) was removed by filtration. The filtrate was added to 50 mL of ice-cold diethyl ether for 2 h. The precipitated product was then redissolved in dichloromethane and reprecipitated with ice-cold diethyl ether. This procedure was repeated at least three times to completely remove excess NHS. Finally, the product was dried under vacuum and stored at room temperature under argon, and then characterized by $^1\text{H-NMR}$ analysis (Bruker AM 400 MHz spectrometer) and Fourier transform-infrared (FT-IR, Thermo Mattson FT-IR spectrometer).

PEI was chemically linked to the GO surface via a condensation reaction between the abundant amino- and carboxyl- groups in their structures.¹⁸ In brief, 20 mg of GO powder was dispersed in 400 mL deionized water by sonication for 2 h, and 4 mmol of EDC and an equal amount of NHS were added to the GO solution in order to activate carboxyl groups of GO. 1 mL of TEA was added to 2 g of PEI solution in 10 mL deionized water. Subsequently, PEI (M_w 1.2 kDa) was added to the GO solution and stirred for 24 h at room temperature. The resulting GO-PEI solution was dialyzed against deionized water using the dialysis tubing with M_w cut-off of 3500 Da for 3 d to remove the unreacted PEI, followed by lyophilized. 242.1 g of GO-PEI was then dissolved in 100 mL deionized water, and 251.4 g of mPEG-NHS was dissolved in 20 mL of anhydrous DMSO. Subsequently, the GO-PEI solution was added to the mPEG-NHS solution, and the reaction was conducted for 24 h at room temperature. The synthesized product was dialyzed against deionized water using the dialysis tubing with M_w cut-off of 3500 Da for 3 d, followed by lyophilized, and characterized by ^1H

NMR and FT-IR.

Preparation of chitosan-aconitic anhydride (CS-Aco) and chitosan-carballylic acid (CS-Car)

30 mg of water-dissolved chitosan was dissolved in 10 mL of 0.5 M NaHCO₃, 393 mg of *cis*-aconitic anhydride or carballylic anhydride powder was then slowly added, and the reaction mixture was stirred for 4 h at 0 °C. The mixture was dialyzed for 2 d against pure water with a dialysis membrane (M_w 3500 Da), and the dialysate was freeze-dried. The resulting white powder dissolved in D₂O for ¹H-NMR analysis.

Assemble of the GO-PEI-PEG/CS-Aco(CS-Car)/PEI/shRNA

After GO-PEI-PEG was coated with CS-Aco or CS-Car, it was collected by centrifuging the mixture twice at 12000 rpm for 20 min and resuspended in 1×PBS buffer. Then, GO-PEI-PEG/CS-Aco (or CS-Car) was coated with PEI for 30 min at room temperature, and the crude complex was purified twice by centrifugation at 12000 rpm for 20 min each. Each complex was resuspended in 1×PBS buffer (pH 7.4). To load shRNA onto the complexes, the solutions of 30 µg/mL shRNA was combined with GO-PEI-PEG/CS-Aco(or CS-Car)/PEI at the indicated vectors/shRNA ratios. The complexes were mixed by pipetting and incubated for 30 min at room temperature.

Zeta potential measurements

The GO based layered nanocomplexes were assembled after each attachment step in PBS buffer (pH 7.4). After each addition, complexes were incubated for 30 min at room temperature, and the zeta potentials were measured by Zetasizer Nano ZS90 (Malvern, UK).

Transmission electron microscopy (TEM) and atomic force microscopy (AFM)

The complexes were treated in PBS buffer (pH 7.4) for 2 h. A drop of complexes solution was deposited on a lacy carbon-coated copper grid. The samples were ready for TEM investigation with a JEOL JEM-2010 (Japan), and then the sample solution was deposited on a mica sheet for 4 h at 37 °C to observe their thickness using AFM (Nano scape IIIA, Veeco).

Loading and release of DOX

Briefly, 10 mg of GO-PEI-PEG or GO was dispersed in 20 mL water by sonication for 2 h, and DOX aqueous solution (0.5 mg/mL) was added. The mixture was continuously sonicated for 30 min and stirred overnight at room temperature. The resulting mixture was centrifuged three times at 12000 rpm for 30 min, and supernatant was disregarded. The resulting solids were redispersed in deionized water, following by freeze-dried. DOX loading capacity of the complex was measured using UV-vis spectrophotometer (Lambda 950 spectrophotometer, Perkin Elmer, USA) at the wavelength number of 490 nm.

The release behavior of DOX was carried out at pH 7.4, 6.8 and 5.0 over a time period of 38 h. In brief, 20 mg of GO-PEI-PEG/DOX/CS-Aco/PEI or GO-PEI-PEG/DOX/CS-Car/PEI was dispersed in 30 mL water, and then 2 mL of the sample solution was further placed into a 24-well plate at different pH in a shaker at 37 °C. In the point time, the solution was taken out from 24-

well plate and centrifuged at 12000 rpm for 30 min. The supernatant containing DOX was further measured by UV-vis spectrophotometer.

shRNA affinity and release from the complexes

Gel electrophoresis assay

The binding capacity of the complexes with shRNA was evaluated by agarose gel electrophoresis assay. The GO-PEI-PEG/CS-Aco/PEI/shRNA complexes at various weight ratios ranging from 1/1 to 10/1 were prepared via the mentioned above method. After incubation, the complexes were loaded on the agarose gel (w/v 1%) containing ethidium bromide (EB) and tris-acetate (TAE) running buffer at 120 V for 30 min. The resulting shRNA migration was analyzed on in vivo imaging (Kodak In-Vivo Imaging System FX Pro).

shRNA release measurement

To evaluate the release of shRNA from the GO-PEI-PEG/CS-Aco/PEI/shRNA nanocomplex at different pH (7.4, 6.5, 5.0), the hybrid/shRNA complexes at weight ratio of 1/6 containing 1 µg of shRNA were cultured in a 96-well plate in a shaker at 37 °C. At selected time intervals, the samples were taken from the plate and centrifuged at 12000 rpm for 30 min. The supernatant containing shRNA was measured using Nano Drop 5000 spectrophotometer (USA).

Cellular uptake

In order to further evaluate the cellular uptake of DOX, DOX was detected by its auto-fluorescence. HepG2 cells were seeded onto a six-well plate at density of 1 × 10⁵ cells with 1 mL growth medium and allowed to culture for 24 h before adding material. The cells were incubated with free DOX, GO/DOX, GO-PEI-PEG/DOX/CS-Aco(or CS-Car)/PEI/shRNA at 37 °C for 4 h. The culture medium was removed and the cells were rinsed three times with PBS to terminate the uptake and remove the drug loaded copolymers absorbed on the cell membrane. The cells were then stained with DAPI in PBS at 37 °C for 10 min and rinsed several times with PBS, and observed by confocal fluorescence microscope (Olympus, Japan).

To investigate the uptake of shRNA in hybrid/shRNA, the complexes were prepared at mass ratio for polymers and YOYO-1 labeled shRNA. HepG2 cells were seeded in a 6-well plate at a density of 1 × 10⁵ cells with 1 mL growth medium and allowed to attach for 24 h. GO-PEI-PEG/CS-Aco(or CS-Car)/PEI were prepared with YOYO-1 at a ratio of 1 nM dye molecule/mg shRNA and incubated for 1 h at room temperature in the dark, and then added onto the cells at a shRNA concentration of 1 mg/well for incubation 4 h at 37 °C. Cells were treated with 14 µM of DAPI and were incubated at 37 °C for additional 10 min, followed by washing with PBS (pH 7.4). Cells were visualized under a confocal fluorescence microscope to observe the internalization of the nanoparticles.

Gene silencing efficiency

shABCG2 cloning

The ABCG2 siRNA sequence 5'-GGUAAGCCA-CUCAUAGAA-3' was cloned into the pSicoR vector with standard procedures (<https://www.addgene.org/12084/>). The

RNA was extracted in the HepG2 cells as described previously (http://tools.lifetechnologies.com/content/sfs/manuals/trizol_reagent.pdf). The detail experimental process was shown in Supporting Information.

Real-time PCR

HepG2 mRNA was then reverse transcribed into cDNA using standard procedures. Gene expression was carried out by real-time quantitative PCR with an ABI 7300 thermal cycler.

Cytotoxicity assay

The cytotoxicity assays were performed with human hepatic (HepG2) cell line by MTS assay. This cell line was seeded into a 96-well plate at a density of 2×10^4 cell/well and maintained at 37 °C in a humidified 5% CO₂ atmosphere using DMEM supplemented with 10% fetal bovine serum (FBS) and 0.1% penicillin-streptomycin for overnight attachment. Subsequently, the old culture media were replaced with 200 μL of fresh media containing PEI (25 kDa), GO-PEI-PEG/CS-Aco/PEI, GO-PEI-PEG/CS-Car/PEI, free DOX, GO/DOX, GO-PEI-PEG/DOX/CS-Aco/PEI, GO-PEI-PEG/DOX/CS-Car/PEI, GO-PEI-PEG/CS-Aco/PEI/shRNA, GO-PEI-PEG/CS-Aco/PEI/ABCG2, GO-PEI-PEG/DOX/CS-Aco/PEI/shRNA and GO-PEI-PEG/DOX/CS-Aco/PEI/ABCG2 at different concentrations. After incubation for 24 h, 20 μL MTS was added to per well. The cell was continuously cultured for 4 h, and measured at 492 nm using a microplate reader (Bio-Tek, Synergy2 and USA). Cell viability was calculated according to: cell viability (%) = $(OD_{\text{treated}}/OD_{\text{control}}) \times 100\%$, where OD_{control} was obtained in the absence of polymer and OD_{treated} was obtained in the presence of polymer.

Results and discussion

Preparation and characterization of GO-PEI-PEG/CS-Aco/PEI

The synthetic route for GO-PEI-PEG and CS-Aco is illustrated in Scheme 2. GO was synthesized according to Hummer's method,¹⁶ followed by covalently linking low molecular weight PEI to GO through amide bond formation by EDC/NHS coupling. The PEI-modified GO was then coupled with mPEG-NHS to improve its stability in the presence of serum, forming a GO-PEI-PEG graft copolymer. GO, GO-PEI and GO-PEI-PEG were characterized through FT-IR spectroscopy, TEM, AFM, and ¹H NMR (Figure S1) measurements. As shown in Figure 1A, the apparent absorption peak at 1723 cm⁻¹ and 3430 cm⁻¹ in the spectra was the characteristic stretching vibrations of C=O in COOH group and -OH bond of GO, respectively. The obvious shifting from the peak at 1723 cm⁻¹ to 1640 cm⁻¹ was observed, indicating the formation N-H bond after the conjugation of PEI. After the GO-PEI nanohybrid was conjugated with PEG, the strong peak at 2886 cm⁻¹ was appeared and corresponding to the symmetric and asymmetric stretching absorbance of methyl of PEG segment. These results suggested that GO-PEI-PEG was successfully prepared. CS-Aco and CS-Car were both successfully synthesized and confirmed by ¹H NMR measurements (Figure S2).

The morphology and thickness of GO-PEI-PEG and GO-PEI-PEG/DOX/CS-Aco/PEI/shRNA were characterized by TEM and AFM (Figure 1B-E). As shown in TEM images (Figure 1B-C), the size of GO-PEI-PEG and GO-PEI-PEG/DOX/CS-

Aco/PEI/shRNA complexes was 250-500 nm and 100-250 nm, respectively, which is much smaller than that of the starting GO sheet (with size of 300-700 nm, Figure S3), indicating the successful chemical conjugation and layer-by-layer condensation on GO sheet. The layered GO-PEI-PEG/DOX/CS-Aco/PEI/shRNA sheets are also found to be more seriously accumulated than GO-PEI-PEG between the graphene layers. The thickness of GO-PEI-PEG and GO-PEI-PEG/DOX/CS-Aco/PEI/shRNA was confirmed by the AFM images (Figure 1D-E). An increase in thickness from 3-5 nm for GO-PEI-PEG to 8-11 nm for GO-PEI-PEG/DOX/CS-Aco/PEI/shRNA suggests that was attributed to the combination of GO-PEI-PEG/DOX, CS-Aco, PEI and shRNA via the electrostatic interactions. These results suggested that GO-PEI-PEG/DOX/CS-Aco/PEI/shRNA nanoparticles were successfully synthesized by the layer-by-layer method.

The surface charge of the GO based nanocomplex was determined with zeta potential after each attachment step of the GO-PEI-PEG/CS-Aco/PEI nanoparticle self-assembly (Table 1). GO-PEI-PEG/CS-Aco complexes with various weight ratios from 1/1 to 1/7 were designed and tested to obtain nanoparticles with the optical negative charge that could be used for the addition of positively charged PEI. The surface charges of GO-PEI-PEG and GO-PEI-PEG/CS-Aco (w/w 1/1) complexes were measured as 9.80 ± 0.98 and 7.41 ± 0.54 mV, respectively. As the weight ratio of GO-PEI-PEG/CS-Aco increased, the surface charge of the complexes changed from positive to negative. The surface charge of GO-PEI-PEG/CS-Aco did not further change when the weight ratio was greater than 1/7. Therefore, GO-PEI-PEG/CS-Aco (w/w 1/7) complexes with a negative surface charge of -8.25 ± 0.56 mV were selected for further assembly with PEI. After the addition of PEI, the surface charge of GO-PEI-PEG/CS-Aco/PEI was slightly positive. These results indicated that CS-Aco and PEI were successfully deposited on the surface of GO-PEI-PEG by the layer-by-layer method.

Loading and binding affinities of DOX and shRNA

In this study, GO-PEI-PEG/CS-Aco/PEI was designed to load and deliver anticancer drugs and shRNA into cancer cells. The loading capacity profile is an important performance indicator of the delivery vehicle. DOX was loaded by sonicating GO-PEI-PEG solution with DOX for 30 min and stirring overnight at room temperature, followed by repeated centrifugation at 12000 rpm for 1 h to remove the free unbound DOX in solution. The color of GO-PEI-PEG/DOX solution changed from yellow to red, suggesting the successful adsorption of DOX on GO-PEI-PEG. The surface charge of GO-PEI-PEG/DOX complexes was also confirmed by zeta potential (Table 1) and the charge of 15.83 ± 0.45 mV was higher than that of GO-PEI-PEG because of the positive charge of DOX. UV-vis spectroscopy of DOX shows an obvious absorption peak at 490 nm which is the characteristic peak of DOX (Figure S4). The formation of GO-PEI-PEG/DOX was further confirmed by UV-vis spectroscopy (Figure 2A). The absorption peak at 490 nm indicates the successful formation of GO-PEI-PEG/DOX composites.

The DOX loading capacity was determined according to the previous method.¹⁹⁻²⁰ The loading capacity of DOX on GO-PEI-PEG was calculated to be about 61% (Figure 2A), which was much higher than the loading ratio of 10% for unmodified GO.

This phenomenon is not same trend as the previously reported GO-polymer hybrids,²¹⁻²² which has lower DOX loading capacity than unmodified GO due to the occupation of GO surface by

polymer. In our study, the chemical conjugation of PEI-PEG on GO has little occupation of the GO surface during the interaction of GO-PEI-PEG with DOX. Furthermore, the good loading

Table 1. Zeta potential of the complexes at different weight ratios.

Complexes	Weight ratio	Zeta potential (mV ± S.D)
GO-PEI-PEG	-	9.80 ± 0.98
GO-PEI-PEG/CS-Aco	1/1	7.41 ± 0.54
GO-PEI-PEG/CS-Aco	1/2	5.10 ± 1.56
GO-PEI-PEG/CS-Aco	1/3	3.42 ± 0.76
GO-PEI-PEG/CS-Aco	1/4	-0.30 ± 0.96
GO-PEI-PEG/CS-Aco	1/5	-3.32 ± 0.62
GO-PEI-PEG/CS-Aco	1/6	-4.62 ± 1.07
GO-PEI-PEG/CS-Aco	1/7	-8.25 ± 0.56
GO-PEI-PEG/CS-Aco	1/8	-8.29 ± 0.53
GO-PEI-PEG/CS-Aco	1/9	-8.98 ± 0.97
GO-PEI-PEG/CS-Aco/PEI	1/7/1	7.63 ± 1.03
GO-PEI-PEG/CS-Aco/PEI	1/7/2	8.11 ± 0.38
GO-PEI-PEG/CS-Aco/PEI	1/7/3	7.70 ± 0.77
GO-PEI-PEG/DOX	-	15.83 ± 0.45
GO-PEI-PEG/DOX/CS-Aco	1/1	12.61 ± 1.17
GO-PEI-PEG/DOX/CS-Aco	1/2	10.11 ± 1.93
GO-PEI-PEG/DOX/CS-Aco	1/3	4.78 ± 1.70
GO-PEI-PEG/DOX/CS-Aco	1/4	0.59 ± 1.59
GO-PEI-PEG/DOX/CS-Aco	1/5	-2.47 ± 1.23
GO-PEI-PEG/DOX/CS-Aco	1/6	-5.47 ± 1.20
GO-PEI-PEG/DOX/CS-Aco	1/7	-7.57 ± 0.93
GO-PEI-PEG/DOX/CS-Aco	1/8	-9.72 ± 0.46
GO-PEI-PEG/DOX/CS-Aco	1/9	-10.40 ± 1.15
GO-PEI-PEG/DOX/CS-Aco	1/10	-10.97 ± 2.44
GO-PEI-PEG/DOX/CS-Aco/PEI	1/8/1	10.97 ± 0.72
GO-PEI-PEG/DOX/CS-Aco/PEI	1/8/2	13.47 ± 2.15
GO-PEI-PEG/DOX/CS-Aco/PEI	1/8/3	13.04 ± 2.70

Note: zeta potential data are presented as mean values ± S.D (n=3).

capacity of GO-PEI-PEG was mainly attributed to the excellent compatibility and solubility enhancement of PEG for DOX, in addition to the π - π stacking, hydrogen bonding and hydrophobic interactions.²³⁻²⁴

The shRNA affinity of the GO-PEI-PEG/CS-Aco/PEI/shRNA nanocomplexes were investigated by agarose gel electrophoresis at various (GO-PEI-PEG/CS-Aco/PEI)/shRNA mass ratios. Figure 2B shows that the migration of shRNA decreased as the mass ratio increased from 1/1 to 10/1. The ratio of 4/1 was sufficient for GO-PEI-PEG/CS-Aco/PEI to condense the shRNA completely.

pH-triggered DOX and shRNA release

To confirm the increase of DOX and shRNA release from the charge-reversible nanocomplex in an acid environment, the release of DOX and shRNA was investigated at pH 7.4, 6.8, and 5.0. The dependence of DOX release on pH values was determined by using a previously reported method,²⁵⁻²⁷ with non-charge-reversible GO-PEI-PEG/DOX/CS-Car/PEI as control. Figure 3A shows that pH-responsive release kinetics were observed for GO-PEI-PEG/DOX/CS-Aco/PEI. DOX release (42% of the total bound DOX) at pH 5.0 was much faster than that at pH 6.8 (27%) and pH 7.4 (23%) after incubation for 38 h. These results suggest that the charge of CS-Aco layer is reversed from negative to positive at a pH of 5.0 through the amide hydrolysis of CS-Aco to CS. The charge reversal causes

electrostatic repulsion between the positive surface charge of DOX, GO-PEI-PEG, CS and PEI, and increases more DOX release than that of in pH of 6.8 and 7.4. Interestingly, non-charge-reversible GO-PEI-PEG/DOX/CS-Car/PEI also displayed similar pH-responsive release behavior, and the DOX release at pH of 5.0 reached 35%, which was higher than that of at pH of 6.8 (24%) and 7.4 (21%). These findings demonstrate that a low pH may accelerate the protonation of amine groups on DOX, and break some of the hydrogen bonds between the -OH and -NH₂ groups in DOX and the -OH groups on GO,²⁸ which increases the hydrophilicity and solubility of DOX and reduces the hydrophobic interactions between DOX and GO-PEI-PEG/CS-Car/PEI, causing more DOX to be released. Although GO-PEI-PEG/DOX/CS-Car/PEI has higher DOX release at pH of 5.0, it shows less 7% than that of GO-PEI-PEG/DOX/CS-Aco/PEI, indicating that to some extent the pH-responsive charge-reversible CS-Aco did enhance the DOX release in low pH environment.

To confirm the release of shRNA from the nanocomplex, (GO-PEI-PEG/CS-Aco/PEI)/shRNA with a mass ratio of 6:1 was incubated at pH 7.4, 6.8, and 5.0. A non-charge-reversible nanocomplex with a similar structure, GO-PEI-PEG/CS-Car/PEI/shRNA, was used as a negative control. Figure 3B shows that after incubation for 12 h, the cumulative amount of shRNA released from the GO-PEI-PEG/CS-Aco/PEI/shRNA complexes was approximately 52% at pH 5.0, 41% at pH 7.4, and 47% at pH

6.8, respectively. The amount of shRNA released from the GO-PEI-PEG/CS-Car/PEI/shRNA complex was 39%, 41% and 42% at pH 7.4, 6.8 and 5.0, respectively, indicating that the release was not strongly dependent on the environmental pH. These results indicate the important role of pH-triggered charge-reversible CS-Aco in increasing the release of DOX and shRNA. The extracellular pH of most tumors is mildly acidic (pH > 6.5), and few tumor environments have a pH < 6.5.²⁹ Therefore, GO-PEI-PEG/DOX/CS-Aco/PEI/shRNA should be stable extracellularly and undergo pH-dependent anticancer drug and shRNA release intracellularly, which might improve the delivery and transfection of anticancer drugs and shRNA.

Cellular uptake

Confocal microscopy was used to provide visual evidence of the cellular uptake of the charge-reversible GO-PEI-PEG/DOX/CS-Aco/PEI/shRNA nanocomplex. GO-PEI-PEG/DOX/CS-Aco/PEI/shRNA was incubated with HepG2 cells, and the cellular uptake was observed by confocal fluorescence microscopy, free DOX, GO/DOX, and GO-PEI-PEG/DOX/CS-Car/PEI/shRNA with equivalent DOX concentrations were used as controls (Figure 4). The mean fluorescence intensity was much higher in the nuclei of cells treated with free DOX after 4 h, and GO/DOX showed a negligible fraction of fluorescence-positive cells. This is because free DOX rapidly accumulates inside the cells and moves into the cell nucleus, whereas the GO-based nanocomplex must first be internalized in cells through endocytosis, and then slowly release DOX before DOX can migrate into the nucleus.⁵ The charge-reversible GO-PEI-PEG/DOX/CS-Aco/PEI/shRNA nanocomplex showed strong fluorescent signals, and the DOX signals in the nucleus were much stronger than those for non-charge-reversible GO-PEI-PEG/DOX/CS-Car/PEI/shRNA, indicating that pH-triggered CS-Aco residues improved DOX delivery efficiency. These results were consistent with the DOX release profiles (Figure 3A).

To examine the intracellular shRNA transport aided by the charge-reversible GO-PEI-PEG/CS-Aco/PEI/shRNA, confocal microscopy was utilized to provide a visual inspection in HepG2 cell for comparison purpose, using (GO-PEI-PEG/CS-Car/PEI)/shRNA complexes as control. As shown in the Figure 5, green fluorescence of YOYO-1 labeled shRNA was clearly detectable within the HepG2 cells. It was found that green fluorescence signals of (GO-PEI-PEG/CS-Aco/PEI)/shRNA in HepG2 cells were much higher than that of the control due to the charge-reversible CS-Aco promoted shRNA release. This result indicated the successful delivery of shRNA to HepG2 cell by the charge-reversible GO-PEI-PEG/CS-Aco/PEI/shRNA.

ABCG2 silencing

After confirming the efficient delivery of the GO-PEI-PEG/CS-Aco/PEI/shRNA complex, we investigated whether this delivery system is a good potential carrier. Herein ABCG2 was used as the target gene due to its critical drug pump action associated with drug resistance. Efficiently silencing the ABCG2 expression usually makes the tumor cells to be more sensitive to anticancer drugs. Therefore, the knockdown efficiency of the ABCG2 protein expression level by GO-PEI-PEG/CS-Aco/PEI/shABCG2 was further investigated with GO-PEI-PEG/CS-Car/PEI/shABCG2, GO-PEI-PEG/CS-Aco/PEI/shRNA and GO-

PEI-PEG/CS-Car/PEI/shRNA as controls. HepG2 cells were transfected with the complexes for 36 h, and the knockdown efficiency of the complexes was confirmed by measuring the expression of ABCG2 with real-time PCR (Figure 6). Real-time PCR results demonstrated that ABCG2 mRNA levels were much lower in HepG2 cells transfected with the GO-PEI-PEG/CS-Aco/PEI/shABCG2 complexes than in cells transfected with the control. GO-PEI-PEG/CS-Aco/PEI/shABCG2 was especially effective under optimal conditions, reducing ABCG2 expression by 25%, compared with the 60% reduction caused by GO-PEI-PEG/CS-Car/PEI/shABCG2. These results suggest that GO-PEI-PEG/CS-Aco/PEI/shABCG2 can effectively silence ABCG2 mRNA levels, resulting from the increase of the transfection efficiency by charge-reversible CS-Aco residues.

Cytotoxicity assay

The biocompatibility of a nanocarrier must be good for delivery applications. Thus, the safety profiles of GO-PEI-PEG/CS-Aco/PEI nanocarrier on HepG2 cells were evaluated using an MTS assay, with GO-PEI-PEG/CS-Car/PEI and PEI (25 kDa) as controls. Figure 7A shows that the cytotoxicity profile of GO-PEI-PEG/CS-Aco/PEI was similar to that of GO-PEI-PEG/CS-Car/PEI at different concentrations after a 48 h treatment, and the cell viability was around or above 90% for all complexes. In contrast, PEI showed highly toxicity at the concentration of 40 $\mu\text{g}/\text{mL}$, and the cell viability decreased to $28 \pm 1.3\%$. Therefore, the modification with biocompatible CS-Aco, PEG, and low molecular weight PEI can greatly reduce the cell cytotoxicity, making the complex suitable as a potential delivery vector.

Then, we evaluated the anticancer effects of DOX loaded on GO-PEI-PEG/CS-Aco/PEI, with controls of free DOX, GO/DOX, and GO-PEI-PEG/DOX/CS-Car/PEI. HepG2 cells were incubated in a medium containing various concentrations of the nanocomplexes with an equivalent concentration of DOX. After 24 h incubation, the relative cell viability was measured by an MTS assay. Figure 7B shows the low cytotoxicity of DOX loaded on GO-PEI-PEG/CS-Aco/PEI compared with free DOX at the same DOX concentration. The decreased cytotoxicity was probably caused by the delayed DOX release from the nanocomplex and the endocytosis mediated cytosolic delivery. Although free DOX showed the most potent anticancer action and is an effective anticancer drug, it is difficult to achieve the minimum effective concentration of DOX and remain below the maximum safe concentration after administration.³⁰ Therefore GO-PEI-PEG/DOX/CS-Aco/PEI could control the delivery of drug molecules. The cytotoxicity of GO-PEI-PEG/DOX/CS-Aco/PEI was higher than that of GO/DOX and GO-PEI-PEG/DOX/CS-Car/PEI, confirming that charge-reversible CS-Aco residues enhanced the DOX release efficiency of the nanocomplexes.

Finally, we investigated the synergistic effect of DOX and shABCG2 by co-delivery of DOX and shABCG2 to HepG2 cells with GO-PEI-PEG/CS-Aco/PEI. HepG2 cells were treated with GO-PEI-PEG/DOX/CS-Aco/PEI/shABCG2 for 24 h, and then an MTS assay was performed to evaluate its cell viability, using GO-PEI-PEG/CS-Aco/PEI/shABCG2, GO-PEI-PEG/CS-Aco/PEI/shRNA and GO-PEI-PEG/DOX/CS-Aco/PEI/shRNA as controls. As shown in Figure 7C, the cellular viability of GO-PEI-PEG/CS-Aco/PEI/shABCG2 and GO-PEI-PEG/CS-

Aco/PEI/shRNA were both about 90% without the addition of DOX. The DOX-loaded GO-PEI-PEG/DOX/CS-Aco/PEI/shABCG2 decreased the cell viability to 26%. However, DOX addition did not largely decrease cell viability for GO-PEI-PEG/DOX/CS-Aco/PEI/shRNA. This result indicated that the efficient shABCG2 delivery and silence of multidrug resistant gene ABCG2 expression by the nanocomplex did improve the sensitivity of HepG2 cells to DOX and the cell cytotoxicity of DOX, which is agree with the previous report.³¹ In summary, the decreased cell viability for GO-PEI-PEG/DOX/CS-Aco/PEI/shABCG2, which contained both DOX and shABCG2, demonstrated the strong synergistic anticancer effect of in vitro study.

Conclusion

In conclusion, we have developed GO-PEI-PEG/DOX/CS-Aco/PEI/shRNA, which is a layered PEI-coated GO nanocomplex interlaid with pH-responsive, charge-reversible CS-Aco, for co-delivery of shRNA and DOX. The nanocomplex exhibits high drug loading and shRNA affinity outside tumor cells at a neutral pH. The charge-reversible CS-Aco changed from negatively to positively charged and facilitated lysosomal rupture and the release of DOX and shRNA into the cytoplasm. The nanocomplex effectively enhanced DOX and shRNA transfection efficiency. Significantly, GO-PEI-PEG/DOX/CS-Aco/PEI/shABCG2 silences multidrug resistant gene ABCG2 expression, and increases the chemotherapy efficacy. This nanocarrier is promising for the co-delivery of DOX and shRNA in vivo, serving as a potential supplement to traditional chemotherapy drug.

Acknowledgments

This work was supported by grants from the National Natural Science Foundation of China (21104029, 21074049), the Gansu Province Science Foundation for Youth (1107RJYA038), Fundamental Research Funds for the Central Universities (Izujbky-2015-22), and Innovation and Entrepreneurship Program of Lanzhou University (20151073001320). We thank Professor Youqing Shen from Zhejiang University very much for help discussion of the rational design for gene delivery vectors.

Notes and references

⁴⁰ Address ¹: State Key Laboratory of Applied Organic Chemistry, Key Laboratory of Nonferrous Metals Chemistry and Resources Utilization of Gansu Province, College of Chemistry and Chemical Engineering, Lanzhou University, Lanzhou, China. Fax: +86-0931-8912144; Tel: +86-0931-8912528; E-mail: lfzhang@lzu.edu.cn

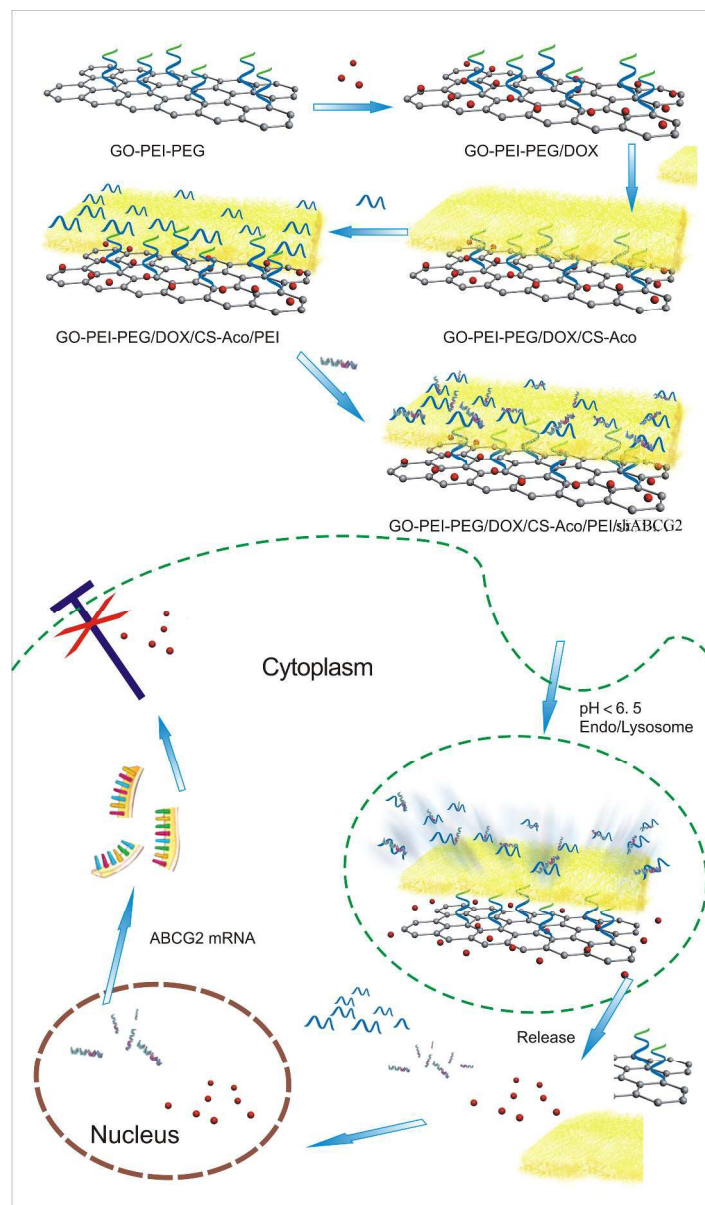
⁴⁵ Address ²: Key Laboratory of Optoelectronic Chemical Materials and Devices of the Ministry of Education, School of Medicine, Institute of Environment and health, Jiangnan University, Wuhan 430056, P.R. China;

Address ³: Lanzhou Jinchuan technology park co., Ltd., Lanzhou, China.

[†]Electronic Supplementary Information (ESI) available: [¹H NMR spectra of GO-PEI, GO-PEI-PEG, CS-Car and CS-Aco, TEM of GO, UV-vis spectroscopy of DOX and the detail process of shABCG2 cloning were investigated]. See DOI: 10.1039/b000000x/.

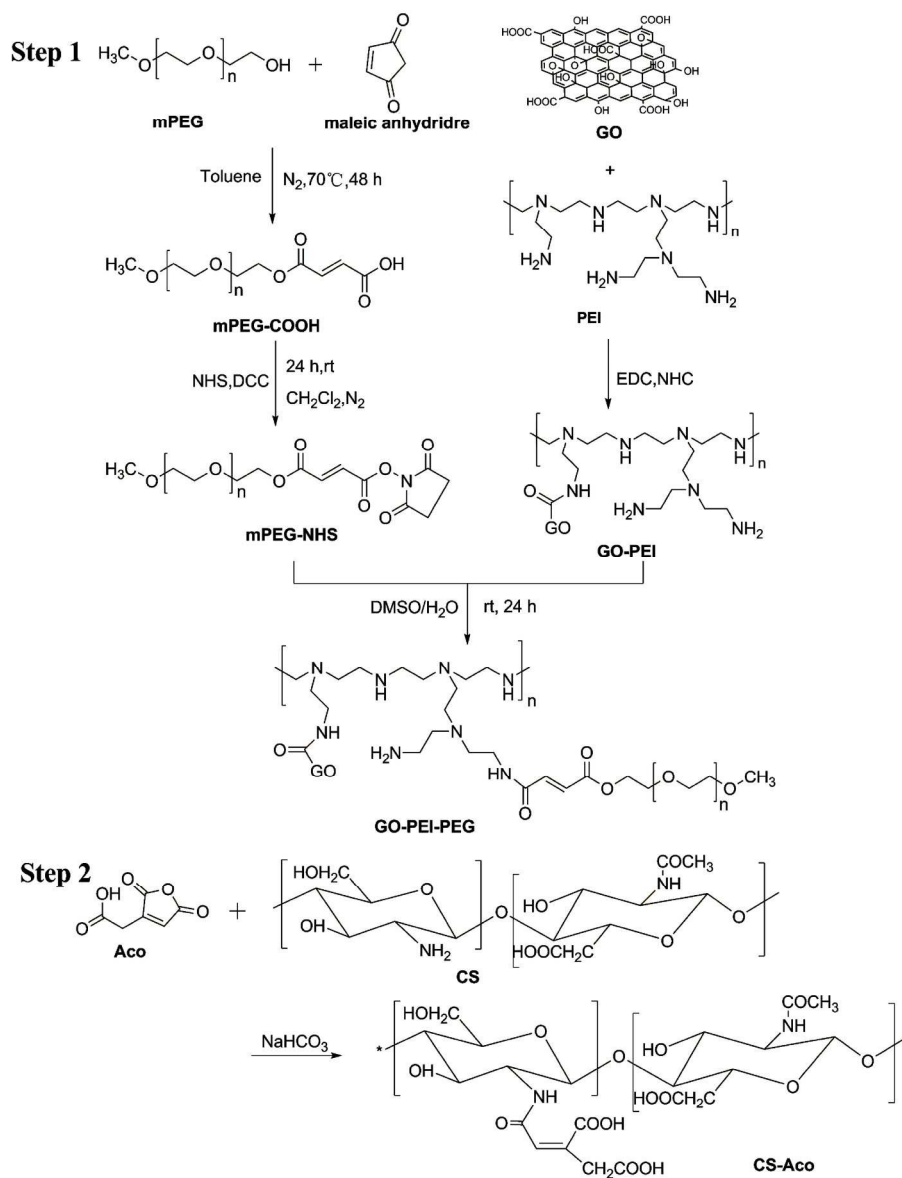
1. G. J. Hannon and J. J. Rossi, *Nature*, 2004, **431**, 371-377.

2. C. Cheng, Z. Liu, H. Zhang, J. Xie, X. Chen, X. Zhao, F. Wang and Y. Liang, *Mol. Cancer Ther.*, 2006, **5**, 2459-2467.
3. M. Dominska and D. M. Dykxhoorn, *J. Cell Sci.*, 2010, **123**, 1183-1189.
4. Y. He, G. Cheng, L. Xie, Y. Nie, B. He and Z. Gu, *Biomaterials*, 2013, **34**, 1235-1245.
5. T. Zhou, X. Zhou and D. Xing, *Biomaterials*, 2014, **35**, 4185-4194.
6. H. Kim, D. Lee, J. Kim, T. I. Kim and W. J. Kim, *ACS Nano*, 2013, **8**, 6735-6746.
7. G. Wu, A. Mikhailovsky, H. A. Khant, C. Fu, W. Chiu and J. A. Zasadzinski, *J. Am. Chem. Soc.*, 2008, **130**, 8175-8177.
8. X. Yang, X. Zhang, Y. Ma, Y. Huang, Y. Wang and Y. Chen, *J. Mater. Chem.*, 2009, **19**, 2710-2714.
9. J. Su, F. Chen, V. L. Cryns and P. B. Messersmith, *J. Am. Chem. Soc.*, 2011, **133**, 1185-1193.
10. X. Yang, Y. Wang, X. Huang, Y. Ma, Y. Huang and R. Yang, *J. Mater. Chem.*, 2011, **21**, 3448-3454.
11. Z. Chen, Y. He, L. Zhang and Y. Li, *J. Mater. Chem. B*, 2015, **3**, 225-235.
12. C. Ding, J. Gu, X. Qu and Z. Yang, *Bioconjug. Chem.*, 2009, **20**, 1163-1170.
13. X. Sun, Z. Liu, K. Welscher, J. T. Robinson, A. Goodwin and S. Zaric, *Nano Res.*, 2008, **1**, 203-212.
14. Z. Liu, J. T. Robinson, X. Sun and H. Dai, *J. Am. Chem. Soc.*, 2008, **130**, 10876-10877.
15. C. Wang, J. Li, C. Amatore, Y. Chen, H. Jiang and X. M. Wang, *Angew. Chem. Int. Ed. Engl.*, 2011, **50**, 11644-11648.
16. W. S. Hummers and R. E. Offeman, *J. Am. Chem. Soc.*, 1958, **80**, 1339-1339.
17. X. Shuai, Z. Jedlinski, Q. Luo and N. Farhod, *Chinese J. Polym. Sci.*, 2000, **18**, 19-23.
18. H. Kim, R. Namgung, K. Singha, I. K. Oh and W. J. Kim, *Bioconjug. Chem.*, 2011, **22**, 2558-2567.
19. M. Wei, R. Yan, D. Dong, X. Wang, J. Zhou and J. Chen, *Chem. Eur. J.*, 2012, **18**, 14708-14716.
20. Z. Liu, X. Sun, N. Nakayama-ratchford and H. Dai, *ACS Nano*, 2007, **1**, 50-56.
21. H. Wang, D. Sun, N. Zhao, X. Yang, Y. Shi, J. Li, Z. Su and G. Wei, *J. Mater. Chem. B*, 2014, **2**, 1362-1370.
22. X. Wang, Q. Han, N. Yu, J. Li, L. Yang, R. Yang and C. Wang, *J. Mater. Chem. B*, 2015, **3**, 4036-4042.
23. L. Zhang, J. Xia, Q. Zhao, L. Liu and Z. Zhang, *Small*, 2010, **6**, 537-544.
24. R. Ghosh, P. Zhang, A. Wang and C. C. Ling, *Angew. Chem. Int. Ed.*, 2012, **51**, 1548-1552.
25. S. Hehir and N. R. Cameron, *Polym. Inter.*, 2014, **6**, 943-954.
26. X. Guan, Y. Li, Z. Jiao, L. Lin, J. Chen, Z. Guo and H. Tian, *ACS Appl. Mater. Interfaces*, 2015, **7**, 3207-3215.
27. Z. Chen, L. Zhang, Y. He, Y. Shen and Y. Li, *Small*, 2014, **11**, 952-962.
28. X. Yang, X. Zhang, Z. Liu, Y. Ma, Y. Huang and Y. Chen, *J. Phys. Chem. C*, 2008, **112**, 17554-17558.
29. K. Engin, D. B. Leeper, J. R. Cater, A. J. Thistlethwaite, L. Tupchong and J. D. McFarlane, *Int. J. Hyperther.*, 1995, **11**, 211-216.
30. J. Liu, S. Guo, L. Han, T. Wang, W. Hong and Y. Liu, *J. Mater. Chem.*, 2012, **22**, 20634-20640.
31. M. R. Dreher, D. Raucher, N. Balu, O. Michael Colvin, S. M. Ludeman and A. Chilkoti, *J. Control. Release*, 2003, **91**, 31-43.



Scheme 1. Schematic representation of GO-PEI-PEG/DOX/CS-Aco/PEI/shABC2 nanocomplexes for intracellular DOX and shABC2 co-delivery. In the endosome, negatively charged CS-Aco could be hydrolyzed into positively charged CS, triggering the electrostatic repulsion between PEI/shABC2 and GO-PEI-PEG/DOX nanoparticles, resulting in the efficient rupture of lysosomes and subsequent DOX and shABC2 release to cytoplasm from short PEI chains. Then, the released shABC2 is expressed and processed by several cellular intrinsic complexes into siABC2, which targeted and cleaved ABCG2 mRNA. Finally, the cleavage of ABCG2 mRNA would largely decrease drug efflux pump activity, enhance the sensitivity of tumor cells to DOX and efficiently improve efficacy of DOX therapy.

237x402mm (300 x 300 DPI)



Scheme 2. Synthesis route of the GO-PEI-PEG and CS-Aco.
184x243mm (300 x 300 DPI)

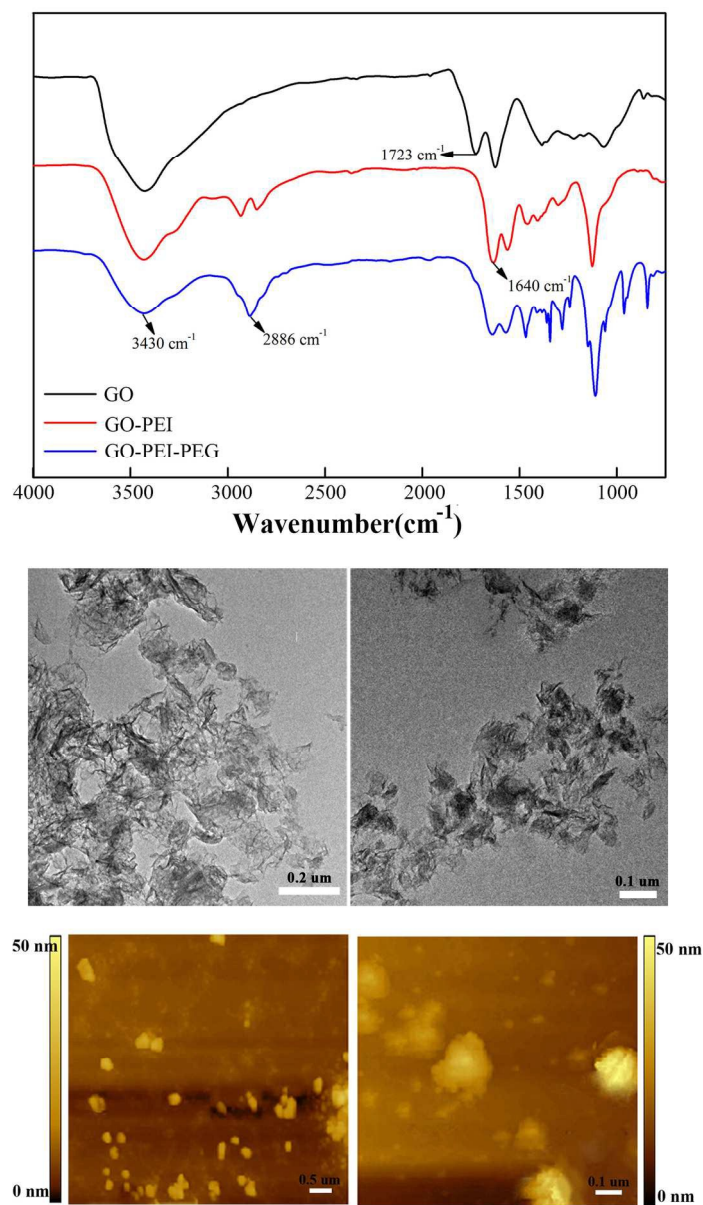


Figure 1. Characterizations of the GO-based nanocomplexes. FT-IR spectra of GO, GO-PEI and GO-PEI-PEG (A); TEM images of (B) GO-PEI-PEG and (C) GO-PEI-PEG/DOX/CS-Aco/PEI/shRNA; AFM images of (D) GO-PEI-PEG and (E) GO-PEI-PEG/DOX/CS-Aco/PEI/shRNA.
122x212mm (300 x 300 DPI)

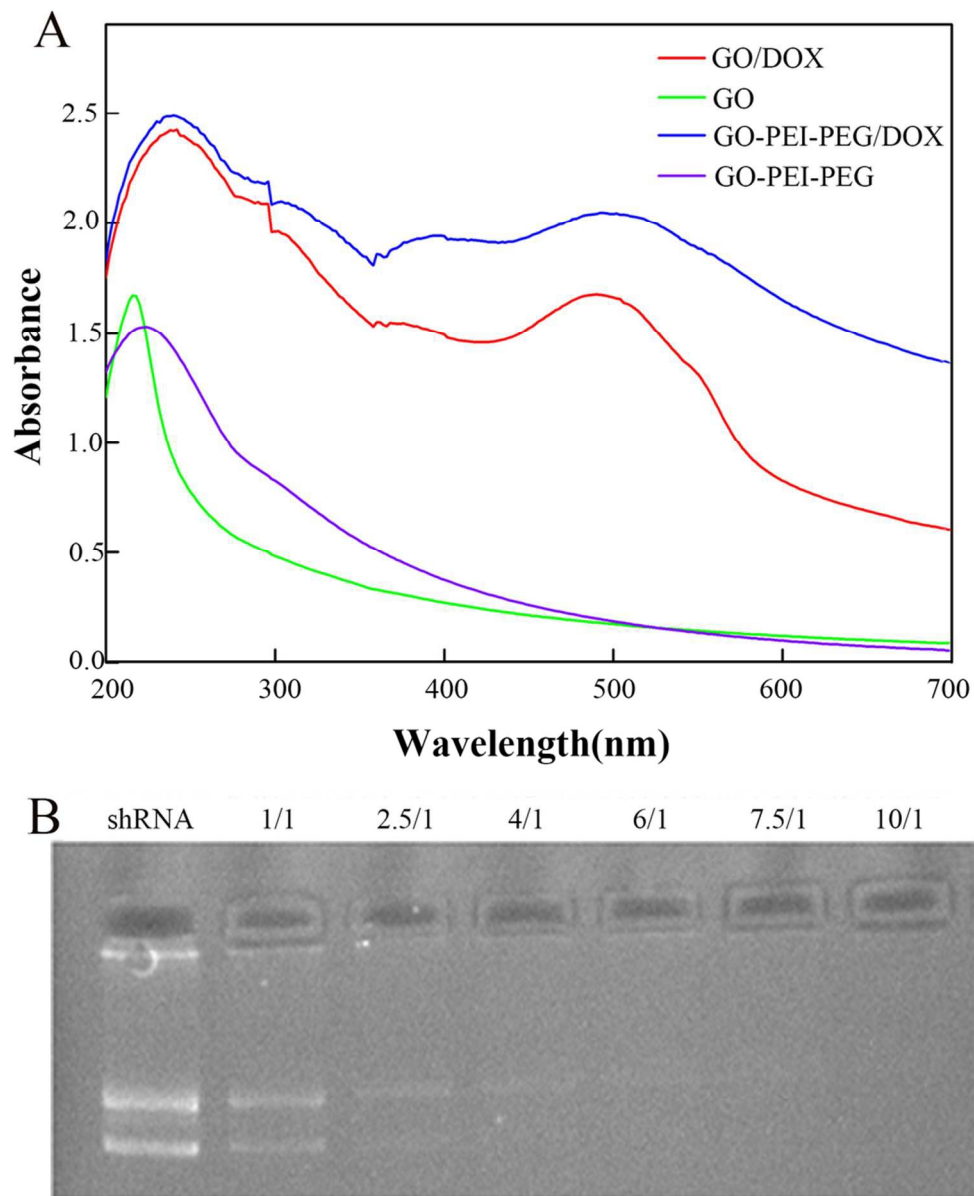


Figure 2. Loading and binding affinities of DOX and shRNA by the complexes. (A) UV-Vis absorbance spectra of GO/DOX, GO-PEI-PEG/DOX, GO and GO-PEI-PEG; (B) Agarose gel electrophoresis retardation assay of (GO-PEI-PEG/CS-Aco/PEI)/shRNA complexes at various weight ratios.
87x109mm (300 x 300 DPI)

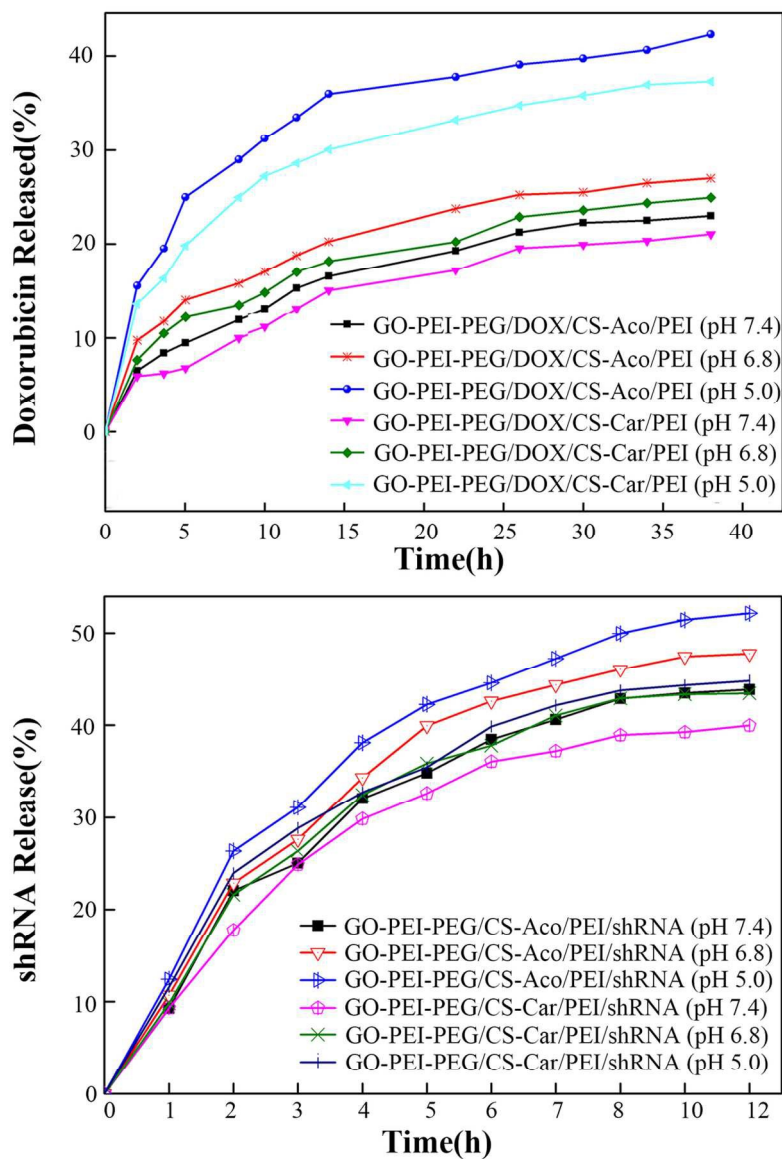


Figure 3. DOX and shRNA release characters of the complexes. Dependence of DOX (A) and shRNA (B) release from the nanocomplexes at different pH value (7.4, 6.8 and 5.0).
104x157mm (300 x 300 DPI)

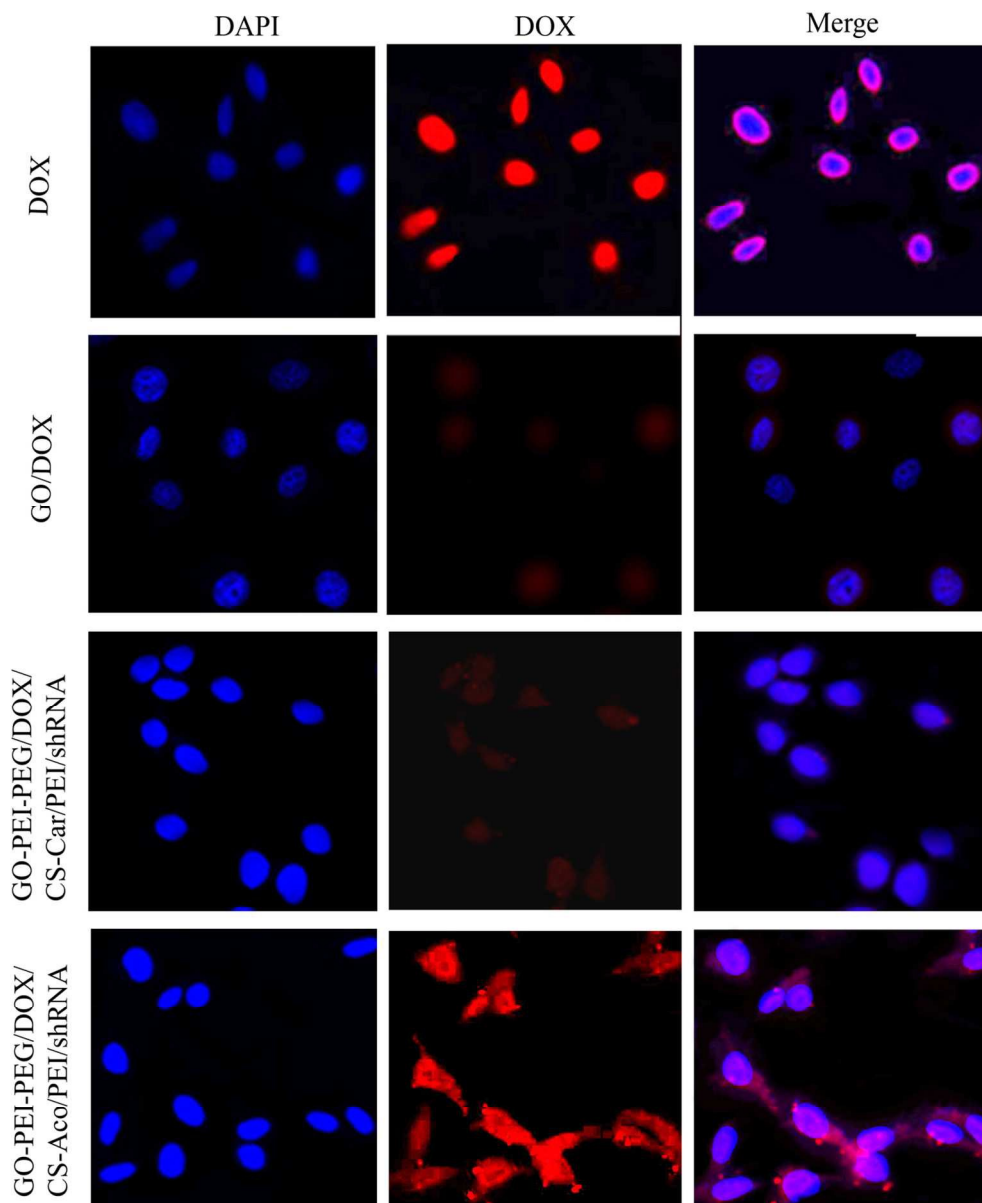


Figure 4. Confocal fluorescence microscopy images of HepG2 cells after treated with free DOX, GO/DOX, GO-PEI-PEG/DOX/CS-Aco/PEI/shRNA and GO-PEI-PEG/DOX/CS-Car/PEI/shRNA after the incubation 4 h (cell nuclei stained by DAPI).
120x145mm (300 x 300 DPI)

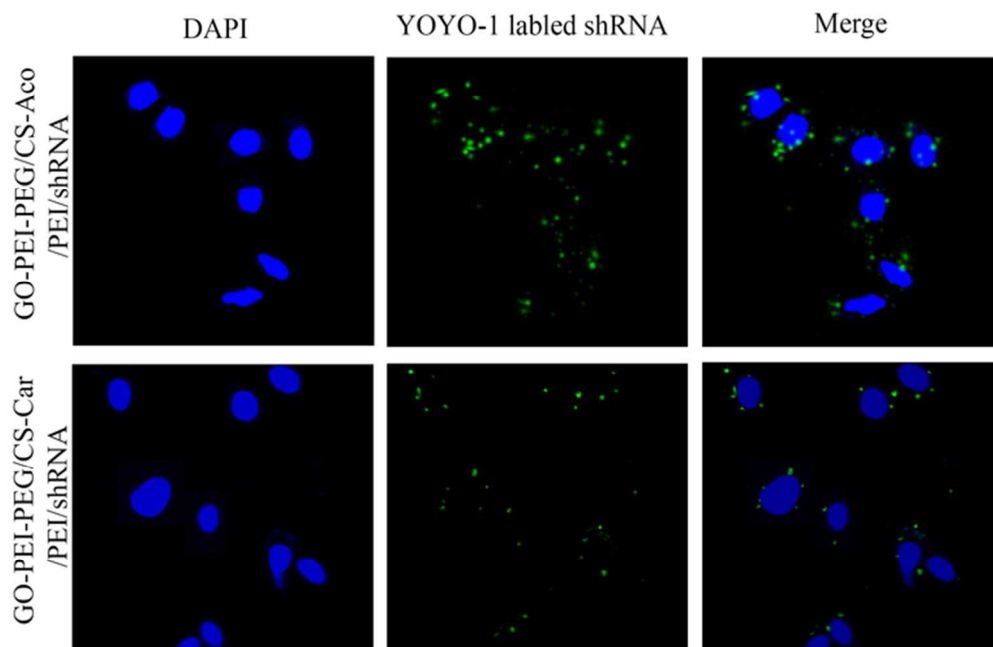


Figure 5. Confocal fluorescence microscopy images of HepG2 cell after the 4 h incubation with (GO-PEI-PEG/CS-Aco/PEI)/shRNA at w/w ratio of 6/1, using (GO-PEI-PEG/CS-Car/PEI)/shRNA as control. shRNA was stained green by YOYO-1, and the nuclei of cell was stained blue by DAPI.
64x42mm (300 x 300 DPI)

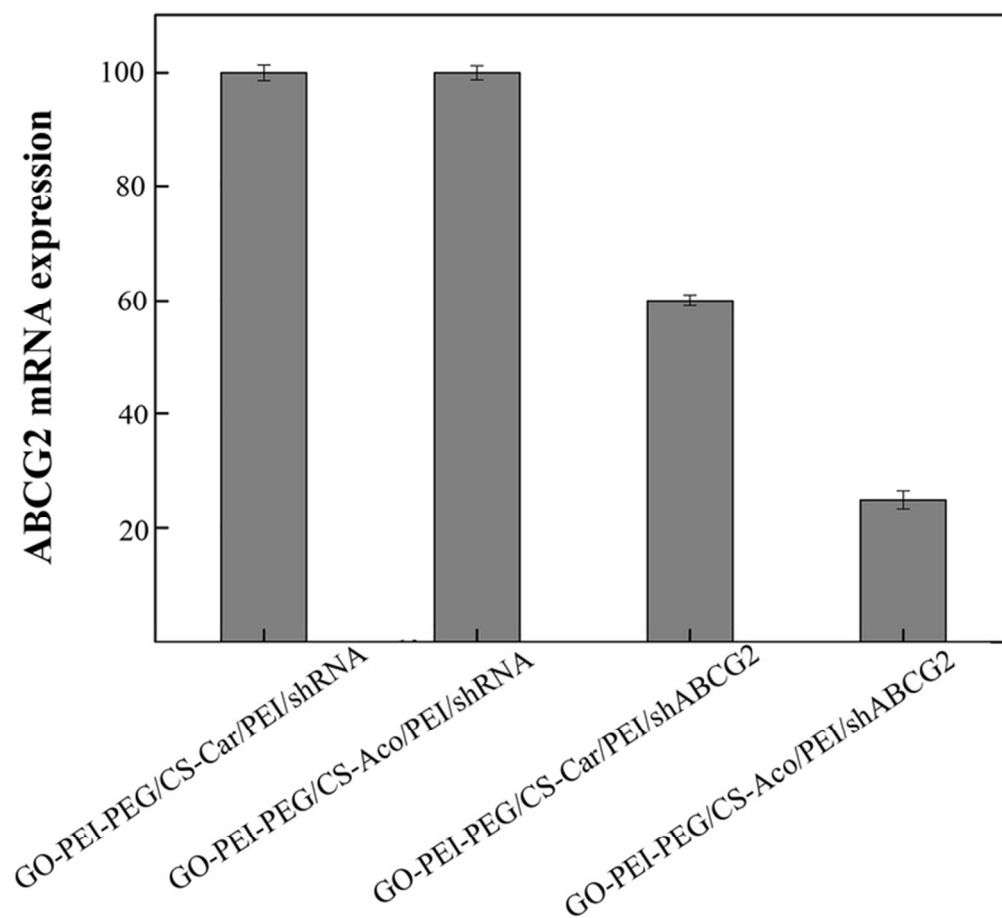


Figure 6. CS-Aco reduced ABCG2 expression. HepG2 cells were treated with different complexes, and knock down efficiency was analyzed by real-time PCR. Data are presented as mean values \pm S.D (n=3). 67x64mm (300 x 300 DPI)

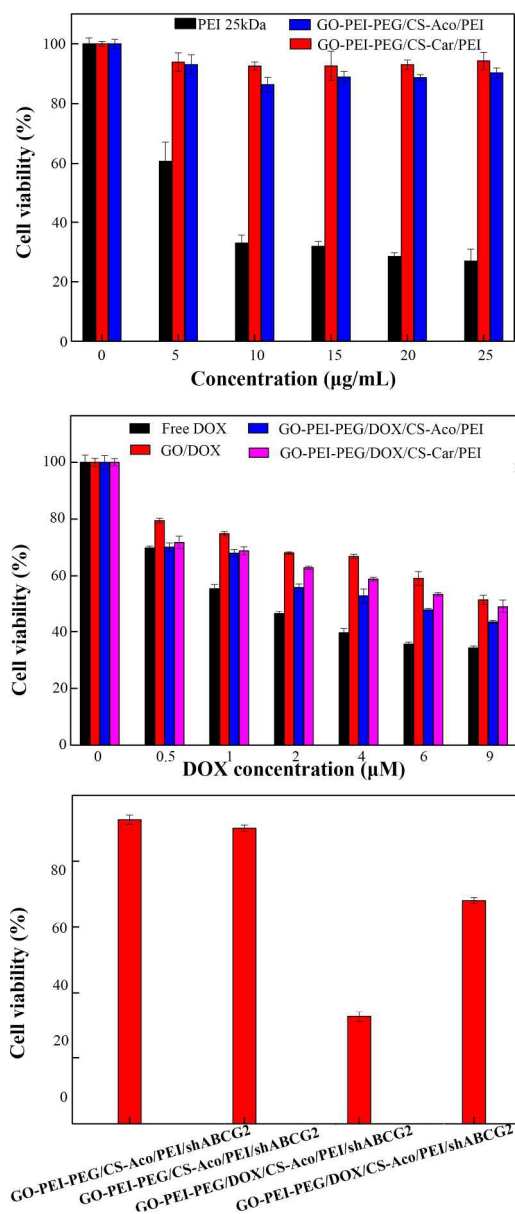
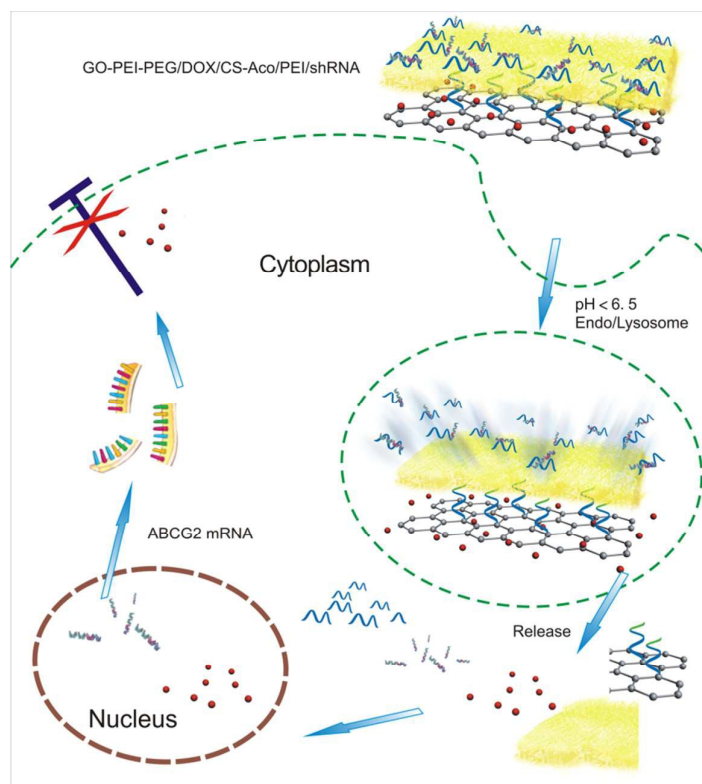


Figure 7. Cellular viability of HepG2 cell was measured by the complexes without DOX (A), with DOX (B), and with both DOX and shABCG2 (C) after treatment for 24 h. Data are presented as mean values \pm S.D (n=3).

164x384mm (300 x 300 DPI)

Graphical abstract



pH responsive charge-reversible GO-PEI-PEG/DOX/CS-Aco/PEI/shABCG2 nanocomplexes for efficient intracellular DOX and shABCG2 co-delivery.